

Supplementary Information

Demonstration of the Photo-controllability of the Bistable Opsin OPN5 using Upconversion Nanoparticles with Multiple Emission Peaks upon Near-infrared Photoexcitation

*Fukue Kotegawa,¹ Mari Takahashi,¹ Koichi Higashimine,² Yuichi Hiratsuka,¹ Kazuaki Matsumura,¹
Daisuke Kojima,³ Shinya Maenosono^{1*}*

¹ School of Materials Science, Japan Advanced Institute of Science and Technology, 1-1 Asahidai, Nomi, Ishikawa 923-1292, Japan

² Center for Nano Materials and Technology, Japan Advanced Institute of Science and Technology, 1-1 Asahidai, Nomi, Ishikawa 923-1292, Japan

³ Department of Biological Sciences, School of Science, The University of Tokyo, 7-3-1 Hongo, Bunkyo-ku, Tokyo 113-0033, Japan

Corresponding Author*

Email: shinya@jaist.ac.jp

Phone: +81-761-51-1611

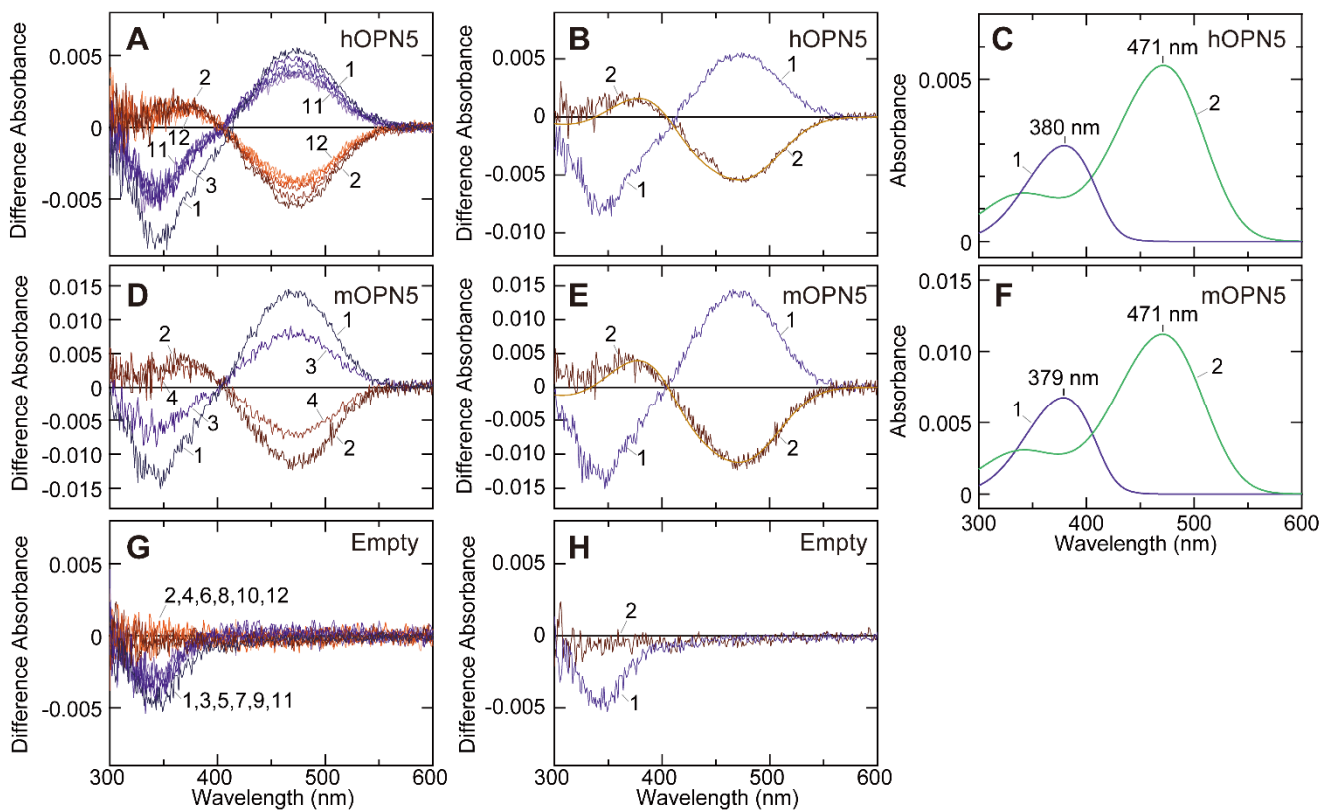


Figure S1. Inference of the absorption spectrum of human OPN5. (A) Spectral changes of recombinant human OPN5 during irradiations. The OPN5 solution was first irradiated with UV light at a wavelength of 357 nm for 4 min, followed by yellow light with a wavelength exceeding 480 nm for 4 min. Difference spectra were obtained by subtracting the spectrum measured at the first dark state from the one measured after UV irradiation (curve 1) and by subtracting the one after UV irradiation from the one after the yellow irradiation (curve 2). (B, C) Inference of human OPN5 spectrum. Curves 1 and 2 in panel C represent the inferred absorption spectra of the inactive state (dark state) and active state (photoproduct) of human OPN5. (D) Spectral changes of recombinant mouse OPN5 during irradiations. The OPN5 solution was first irradiated with UV light at a wavelength of 357 nm for 16 min, followed by orange light with a wavelength exceeding 520 nm for 4 min. Difference spectra were obtained by subtracting the spectrum measured at the first dark state from the one measured after UV irradiation (curve 1) and by subtracting the one after UV irradiation from the one after the orange irradiation (curve 2). (E, F) Inference of mouse OPN5 spectrum. (G, H) Spectral changes for the membrane extract for HEK293S cells having no OPN5 protein during repeated and alternated irradiation with UV (curves 1, 3, 5, 7, 9 and 11) and yellow light (curves 2, 4, 6, 8, 10 and 12) as in panel A. Reprinted from *PLoS ONE* 6(10): e26388,¹ under a CC BY license.

EXPERIMENTAL SECTION

Chemicals

Yttrium(III) chloride hexahydrate ($\text{YCl}_3 \cdot 6\text{H}_2\text{O}$), ytterbium(III) chloride hexahydrate ($\text{YbCl}_3 \cdot 6\text{H}_2\text{O}$), thulium(III) chloride hexahydrate ($\text{TmCl}_3 \cdot 6\text{H}_2\text{O}$), lutetium(III) chloride hexahydrate ($\text{LuCl}_3 \cdot 6\text{H}_2\text{O}$), ammonium fluoride (NH_4F , purity > 99.99%), sodium hydroxide (NaOH , purity > 98%), and oleic acid (purity 90%) were purchased from Sigma-Aldrich. 1-octadecene (purity 90%) was purchased from Kanto Chemical. 1,2-Dioleoyl-*sn*-glycero-3-phosphoethanolamine-*N*-(biotinyl) (sodium salt) (biotin-DOPE) and 1,2-dioleoyl-*sn*-glycero-3-phosphoethanolamine-*N*-(methoxy(polyethylene glycol)-350) (ammonium salt) (DOPE-PEG350) were purchased from Avanti Polar Lipids. HEK293T cell line was purchased from RIKEN BioResource Research Center. Alexa Fluor 568-labelled streptavidin (#S11226), lipofectamine 2000, and acetoxymethyl Fluo-4 were obtained from Invitrogen. ANTI-FLAG BioM2-biotin antibody (#F9291), monoclonal ANTI-FLAG M2 antibody (#F1804) and poly(L-lysine) solution (0.01%) were purchased from Sigma-Aldrich. Goat anti-mouse IgG (H+L) cross-adsorbed secondary antibody with Alexa Fluor 594 (#A-11005) was obtained from Invitrogen. Hanks' balanced salt solution (HBSS, phenol red-free, Ca^{2+} containing) and Dulbecco's modified eagle medium (DMEM) were purchased from Nacalai Tesque. Fetal bovine serum (FBS) was purchased from biosera. Dulbecco's phosphate-buffered saline (PBS) was prepared by dissolving AccuDia D-PBS(-) powder (Shimadzu Diagnostics Corp.) in pure water and sterilizing it in an autoclave before use. 11-*cis*-retinal (purity > 65%) was obtained from FUJIFILM Wako Pure Chemical. Calcium ionophore (calcimycin) was purchased from Sigma-Aldrich. All chemicals were used without further modification.

Synthesis of core-shell UCNPs

In this study, we modified the method of Youn *et al.*² to synthesise $\text{NaYF}_4:\text{Yb,Tm}@\text{NaLuF}_4$ core-shell UCNPs. First, the core $\text{NaYF}_4:\text{Yb,Tm}$ UCNPs were synthesised. 8 mL of methanol (MeOH), 0.5 mmol of $\text{YCl}_3 \cdot 6\text{H}_2\text{O}$, 0.497 mmol of $\text{YbCl}_3 \cdot 6\text{H}_2\text{O}$, and 0.003 mmol of $\text{TmCl}_3 \cdot 6\text{H}_2\text{O}$ were added to a 100-mL three-necked flask, and the mixture was stirred under an argon gas flow at room temperature until all the precursors were sufficiently dissolved in MeOH. A mixture of 8 mL of oleic acid and 15 mL of 1-octadecene was added to the flask, and the temperature was raised to 160°C and held for 30 min. The reaction solution was then allowed to cool naturally to room temperature, and a solution of NH_4F (4 mmol) and NaOH (2.5 mmol) in MeOH (20 mL) was added to the flask. The temperature was raised to 120°C again to evaporate volatile components such as MeOH, and then held for 30 min while stirring. The reaction temperature was then increased to 317°C and the reaction was allowed to continue for 10 min under reflux conditions, after which the mixture was allowed to cool naturally to room temperature. After the reaction had finished, excess ethanol was added to the reaction mixture and the mixture was centrifuged at 2,000 $\times g$ for 5 min. The precipitate was washed once with chloroform/ethanol (1:10 v/v) and twice with cyclohexane/acetone (1:10 v/v). Finally, the resulting UCNPs were redispersed in cyclohexane, centrifuged at 1,500 $\times g$ for 5 min, and the supernatant was collected. Acetone was added, and the mixture was centrifuged at 4,000 $\times g$ for 10 min to obtain the core $\text{NaYF}_4:\text{Yb,Tm}$ UCNPs.

Next, the following procedure was used to form a NaLuF_4 shell on the surface of the $\text{NaYF}_4:\text{Yb,Tm}$ core. We placed 0.5 mmol of $\text{LuCl}_3 \cdot 6\text{H}_2\text{O}$ and 8 mL of MeOH in a 100 mL three-necked flask and stirred at room temperature with argon bubbling until dissolved. Subsequently, a mixture of oleic acid (8 mL) and 1-octadecene (15 mL) was added to the flask, the temperature was raised to 160°C and held for 30 min. The reaction solution was then allowed to cool naturally to room temperature, after which 25 mL of a chloroform dispersion of $\text{NaYF}_4:\text{Yb,Tm}$ core UCNPs (concentration 1 mg/mL) was added to the flask. The temperature was then raised to approximately 110°C, and after the volatile components such as

chloroform had completely evaporated, the mixture was allowed to cool naturally to room temperature. A solution of NH₄F (2 mmol) and NaOH (1.25 mmol) in MeOH (10 mL) was then added to the flask, the temperature raised to 120°C, and held for 30 min. The reaction temperature was then increased to 317°C and the reaction was allowed to continue for 10 min under reflux conditions, after which the mixture was allowed to cool naturally to room temperature. The washing process was carried out in the same way as for NaYF₄:Yb,Tm core UCNPs, and NaYF₄:Yb,Tm@NaLuF₄ core-shell UCNPs were obtained.

Structural analysis and optical property evaluation of UCNPs

The structures of the as-synthesised core and core-shell UCNPs were analysed using a transmission electron microscope (TEM, Hitachi H-7650) at an acceleration voltage of 100 kV and X-ray diffraction (XRD, Rigaku MiniFlex600) using Cu K α line (1.5418 Å). Furthermore, for the core-shell UCNPs, we used a scanning TEM equipped with energy-dispersive X-ray spectroscopy (EDS) and a high-angle annular dark-field (HAADF) detector (STEM, JEOL JEM-ARM200F) at an acceleration voltage of 200 kV to confirm that the shells were properly formed. The emission spectra of the UCNPs were obtained using a near-infrared diode laser (PGL-V-H-980-1W, Changchun New Industries Optoelectronics Tech. Co., Ltd., wavelength 980 nm, output power 1084 mW) as the excitation light source, and a fluorescence spectrophotometer (FP-6300, Jasco).

Encapsulation of UCNPs with phospholipids

Since the as-synthesised UCNPs are hydrophobic, they were encapsulated using phospholipid micelles, as reported in previous studies.^{3,4} To explain briefly, 840 µL of a chloroform solution of biotin-DOPE (5.5 mM) and 210 µL of a chloroform solution of DOPE-PEG350 (5.5 mM) were added to a two-necked flask and mixed well by pipetting. Next, 2.8 mL of a chloroform dispersion of freshly prepared UCNPs (1 mg/mL) was added to a two-necked flask and mixed well by repeated pipetting. After that, the chloroform was completely evaporated under an argon gas flow. The resulting dried solid was redispersed in pure water, centrifuged at 11,000 \times g for 10 min, and the supernatant was removed. The precipitate was redispersed in pure water and the water-dispersible UCNPs encapsulated with biotin-DOPE and DOPE-PEG350 were obtained (hereafter referred to as UCNP@Biotin). The zeta potential and hydrodynamic diameter of UCNP@Biotin were measured using a Zetasizer Nano ZS (Malvern).

OPN5 plasmid construction

A plasmid encoding human OPN5 with an extracellular FLAG tag was constructed using the Snorkel system (Figure S2a).⁵ Specifically, the Snorkel extends from the C-terminus of OPN5, passes through the cell membrane, and presents the FLAG tag on the extracellular surface. The transmembrane topology of OPN5 expressed from the plasmid in this study was predicted by DeepTMHMM (Figure S2b).⁶ This result confirmed that the structure of OPN5 was as designed, and that FLAG was exposed to the extracellular space by Snorkel. The commercially available human OPN5 plasmid (GPR136 (OPN5) (NM_181744) Human Tagged ORF Clone, OriGene) was used as the source of the OPN5 coding sequence and the vector backbone. The DNA sequence encoding the Snorkel domain was synthesised by Eurofins Genomics based on a published design. The three fragments, (1) OPN5 coding sequence, (2) vector backbone, and (3) Snorkel domain, were amplified by PCR. These fragments were then assembled by ligation using EcoRI and AgeI restriction enzyme sites. The complete plasmid construct was sequence-verified using whole-plasmid sequencing based on Oxford Nanopore technology (Eurofins Genomics, Japan).

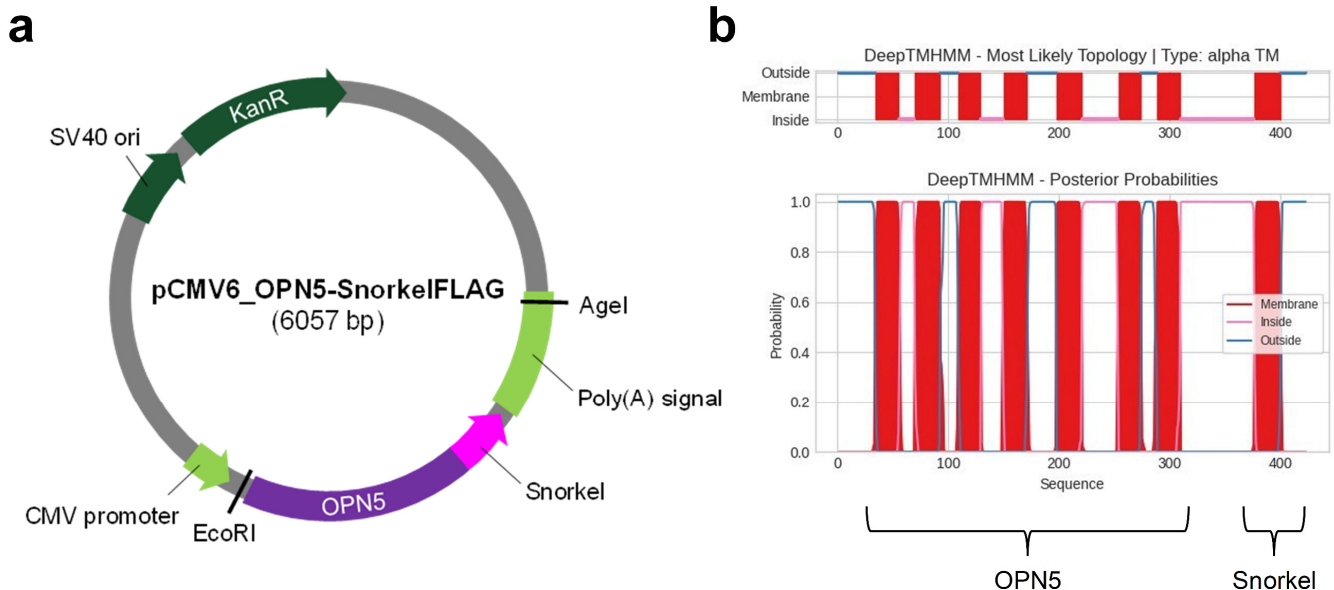


Figure S2. (a) Plasmid map. (b) Transmembrane topology of OPN5, expressed from our plasmid (pCMV6_OPN5-SnorkelFLAG), predicted by a deep learning protein language model-based algorithm (DeepTMHMM⁶).

Creation of OPN5-expressing cells

For all cell experiments, we used the HEK293T cell line, which stably expresses the large T antigen of simian virus 40 (SV40) and has high transfection efficiency.⁷ For transient expression of OPN5, 2×10^5 cells/dish were seeded in 35-mm-diameter dishes containing DMEM with 10% FBS. After 24 hours of incubation, the OPN5 plasmid (0.2 μ g/dish) was transfected into the cells using 0.8 μ L/dish of Lipofectamine 2000 (corresponding to a 1:4 (w/v) ratio of DNA to Lipofectamine), and the cells were incubated for a further 24 hours at 37°C in 5% CO₂, after which they were used in the subsequent experiments.

Binding of UCNPs to cells

UCNP@Biotin was bound to OPN5-expressing HEK293T cells (OPN5-HEK) via the FLAG tag (Figure S3). At 24 hours after the transfection of the OPN5 plasmid, ANTI-FLAG BioM2–Biotin antibody (1 mg/mL) was diluted 250 times in HBSS with 0.1% BSA, and 1 mL of the solution was added to the cells. The cells were then shaken for 5 min, allowed to stand for 1 min, and washed once with 1 mL of HBSS (0.1% BSA). Next, 1 mL of a HBSS (0.1% BSA) solution of Alexa Fluor 568-labelled streptavidin (5 μ g/mL) was added to the dish. The dish was then shaken for 4 min, left to stand for 1 min, and washed twice with 1 mL of HBSS (0.1% BSA). Subsequently, a dispersion of 200 μ g UCNP@Biotin dispersed in 1 mL DMEM (–FBS) was added to the dish, which was then shaken for 3 min, and allowed to stand in the incubator at 37 °C, in 5% CO₂ for 2 min. Finally, the cells were washed twice with DMEM (–FBS).

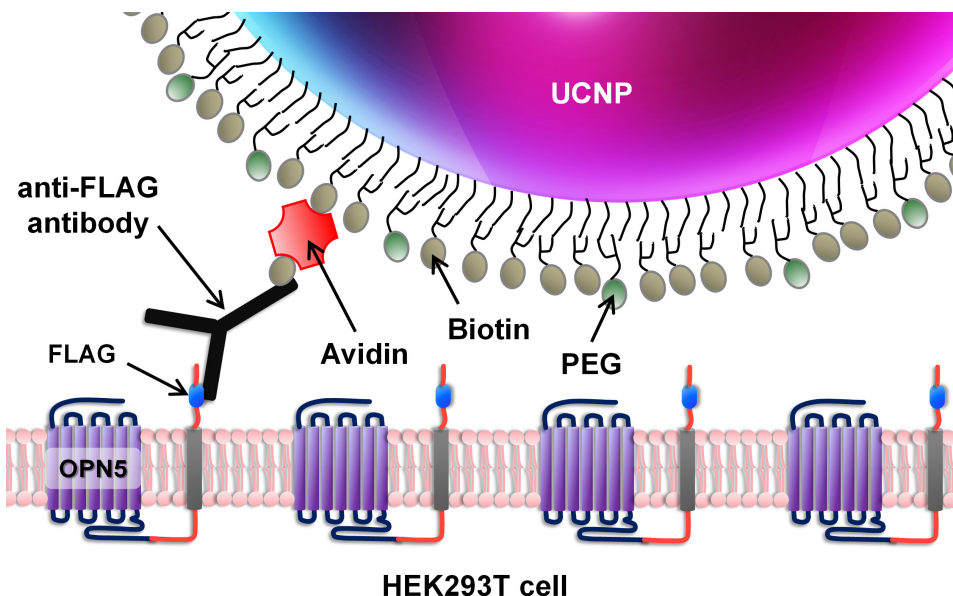


Figure S3. Schematic illustration of the binding of a UCNP@Biotin to an OPN5-HEK.

Immunofluorescence microscopy

We performed immunostaining to estimate the transfection efficiency and to confirm that FLAG was expressed in the extracellular domain by the Snorkel. As the primary antibody, we added an anti-FLAG antibody (Monoclonal ANTI-FLAG M2) (1 mg/mL) dissolved in PBS (3% BSA) at a dilution rate of 1:2000 to the dish. We then added Goat anti-Mouse IgG (H+L) Cross-Adsorbed Secondary Antibody with Alexa Fluor 594 (2 mg/mL) ($\lambda_{\text{ex}}/\lambda_{\text{em}} = 590/618$ nm) dissolved in PBS (3% BSA) at the same dilution rate of 1:2000 and observed the dish under a fluorescence microscope (BZ-810, KEYENCE). Fluorescence microscope observation was carried out using a TRITC filter ($\lambda_{\text{ex}}/\lambda_{\text{em}} = 545\pm25/605\pm70$ nm). For estimating the transfection efficiency, immunostaining was performed with membrane permeabilization, but for estimating the percentage of cells expressing FLAG in the extracellular domain, immunostaining was performed without membrane permeabilization. Those percentages were estimated by dividing the number of cells emitting fluorescence by the total number of cells.

Next, we tried to confirm whether UCNP@Biotin was bound to FLAG, but when we irradiated the cells with an NIR laser (wavelength 980 nm, output power 1084 mW) and observed the resulting fluorescence through a DAPI filter ($\lambda_{\text{ex}}/\lambda_{\text{em}} = 360\pm20/460\pm25$ nm), we were unable to clearly capture the UCNP emission because it was obscured by the scattered light of the second harmonic of the NIR laser light.

Ca²⁺ imaging

Before seeding the cells, the 35-mm dishes were coated with poly(L-lysine). OPN5-HEK were prepared as described previously. After 10 hours of transfection with the plasmid, the medium was replaced with 2 mL of DMEM (10% FBS) containing 11-cis-retinal (1 μ M). After 14 hours, UCNP@Biotin was bound to the cells using the aforementioned method, and 1 mL of HBSS containing acetoxyethyl Fluo-4 (2 μ M), a Ca²⁺ indicator, was added. The relative intracellular Ca²⁺ concentration was measured by observing the fluorescence intensity of Fluo-4 using the fluorescence microscope with a GFP filter ($\lambda_{\text{ex}}/\lambda_{\text{em}} = 470\pm40/525\pm50$ nm). Fluorescence microscope images were taken every 10 seconds, and the excitation light was turned on 1 min and 1 sec after the start of image acquisition, and turned off 1 min and 9 sec later (in order to avoid overlapping image acquisition and excitation light irradiation). The average value of the fluorescence intensity for the 1 min before light stimulation was defined as F_0 , and the cells that

showed an increase in fluorescence intensity, $F(t)$, of $\geq 1.2F_0$ were defined as “responding cells”. From the obtained fluorescence microscope images, all responding cells were selected, and the time variation in $F(t)$ of each cell was tracked using image analysis with the ImageJ software. Excitation of UCNPs bound to OPN5-HEK was performed using a NIR laser (wavelength 980 nm, output power 1084 mW). In the control experiment, a UV LED (ZUV-L 10H, OMRON) (wavelength 365 nm, output power 45 mW/cm²) was used to activate OPN5 by irradiating UV light directly onto OPN5-HEK. After the Ca²⁺ imaging experiment, 10 μ M of calcimycin was added to the culture dish, and the fluorescence intensity of Fluo-4 was allowed to reach saturation before taking a picture with a fluorescence microscope to estimate the upper limit of the Ca²⁺ concentration in HEK293T cells in this experimental system.

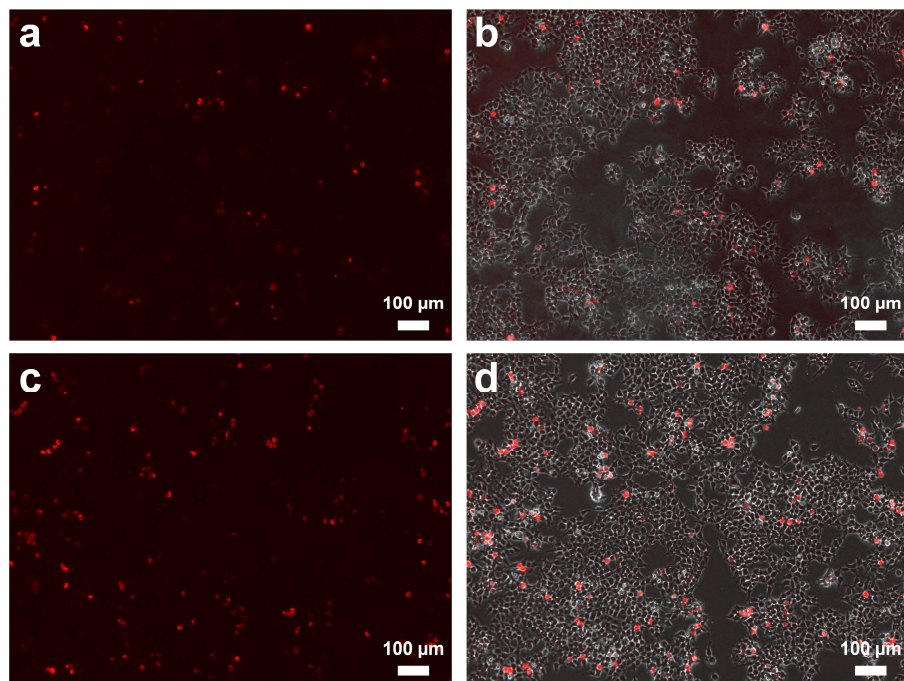


Figure S4. Fluorescence image of OPN5-HEK (left) and merged image of fluorescence and phase images (right), immunostained with a primary antibody (anti-FLAG antibody) and an Alexa Fluor 594-labelled secondary antibody (IgG). (a,b) Without and (c,d) with membrane permeabilization.

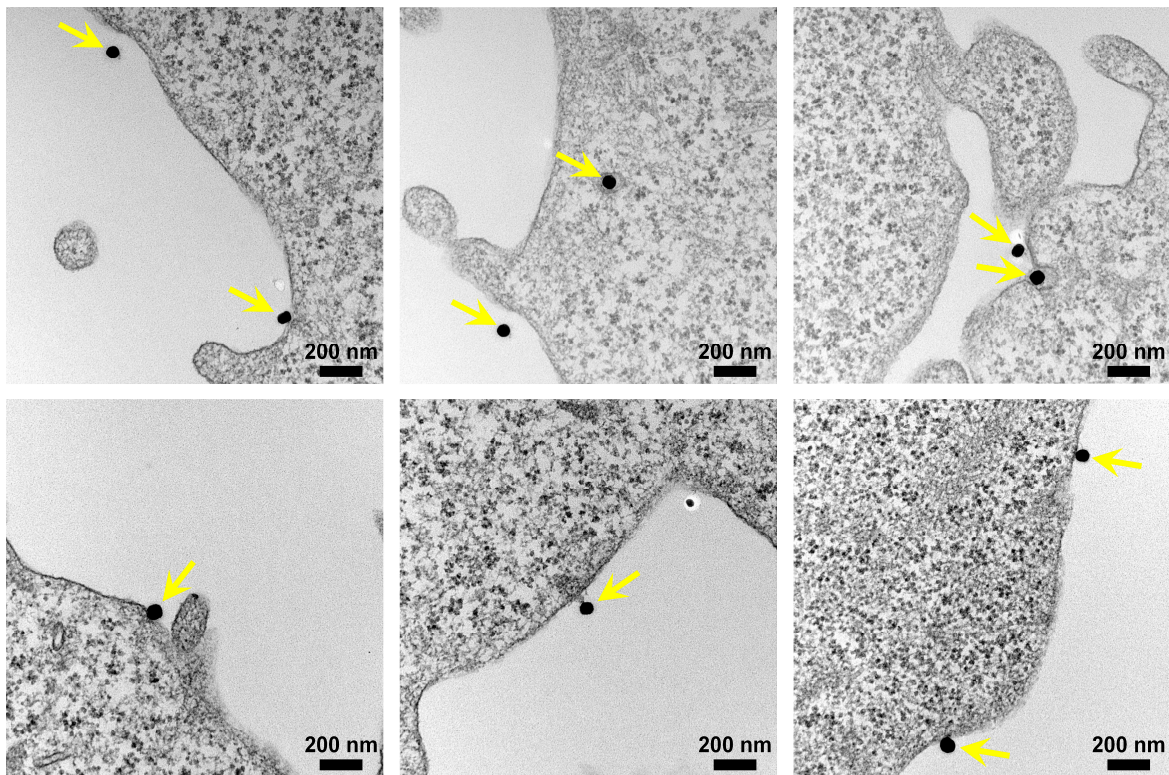


Figure S5. TEM images of OPN5-HEK sequentially conjugated with biotinylated anti-FLAG antibody, streptavidin, and UCNPs@Biotin. UCNPs@Biotin was bound to OPN5-HEK as described in the protocol on p. S5. UCNPs are indicated by yellow arrows. The small black dots visible throughout the cell are free ribosomes. After binding UCNPs@Biotin to OPN5-HEK, the cells were fixed in phosphate-buffered 2% glutaraldehyde at 4°C and postfixed in 2% osmium tetra-oxide for 3 h in an ice bath, followed by dehydration in ethanol before being embedded in epoxy resin. The ultrathin section obtained by an ultramicrotome technique was stained with uranyl acetate for 10 min and lead-staining solution for 5 min before TEM observation (JEM-1200 EX, JEOL).

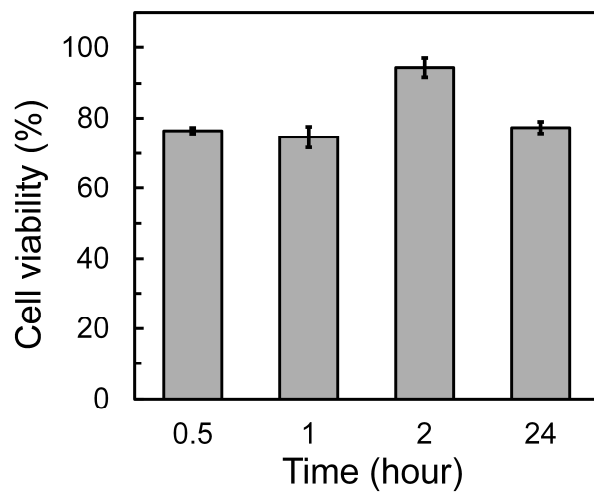


Figure S6. Results of the MTT assay for UCNPs@Biotin. HEK293T cells were seeded into a 96-well plate (1×10^4 cells per well, DMEM containing 10% FBS) and cultured for 1 day at 37°C in a 5% CO₂ incubator. UCNPs@Biotin was dispersed in DMEM containing 10% FBS and added to the wells at a final concentration of 200 µg/mL. After 0.5, 1, 2, and 24 hours of culture, MTT solution (Dojindo Ltd., prepared in FBS-free DMEM) was added to the wells. The medium was removed, and the formazan crystals were dissolved in dimethyl sulfoxide. Absorbance was measured at 540 nm using a microplate reader (Infinite M Nano, TECAN).

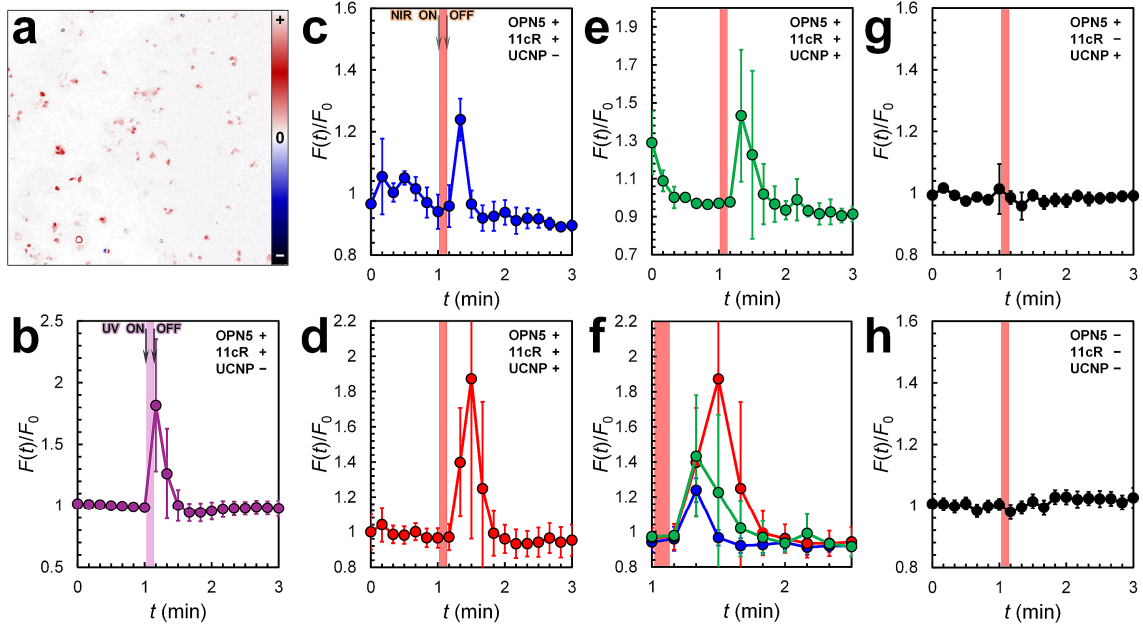


Figure S7. Results of the second replication experiment for Ca^{2+} imaging. (a) Difference fluorescence images before and after UV irradiation of OPN5-HEK (after – before). Note that the post-irradiation fluorescence image refers to the fluorescence image captured 1 second after the completion of UV irradiation. (b) \bar{F} when OPN5-HEK (-UCNP) was irradiated with UV light, (c) \bar{F} when OPN5-HEK (-UCNP) was irradiated with NIR light, (d) \bar{F} when OPN5-HEK (+UCNP (bound)) was irradiated with NIR light, and (e) \bar{F} when OPN5-HEK (+UCNP (unbound)) was irradiated with NIR light. (f) Graph plotted by overlaying panels c-e. (g) Average $F(t)/F_0$ for 100 randomly-selected cells in OPN5-HEK (+UCNP (bound), -11cR) when irradiated with NIR light ($N_{\text{responding}} = 0$), and (h) average $F(t)/F_0$ for 100 randomly-selected cells in HEK293T cells when irradiated with NIR light ($N_{\text{responding}} = 0$).

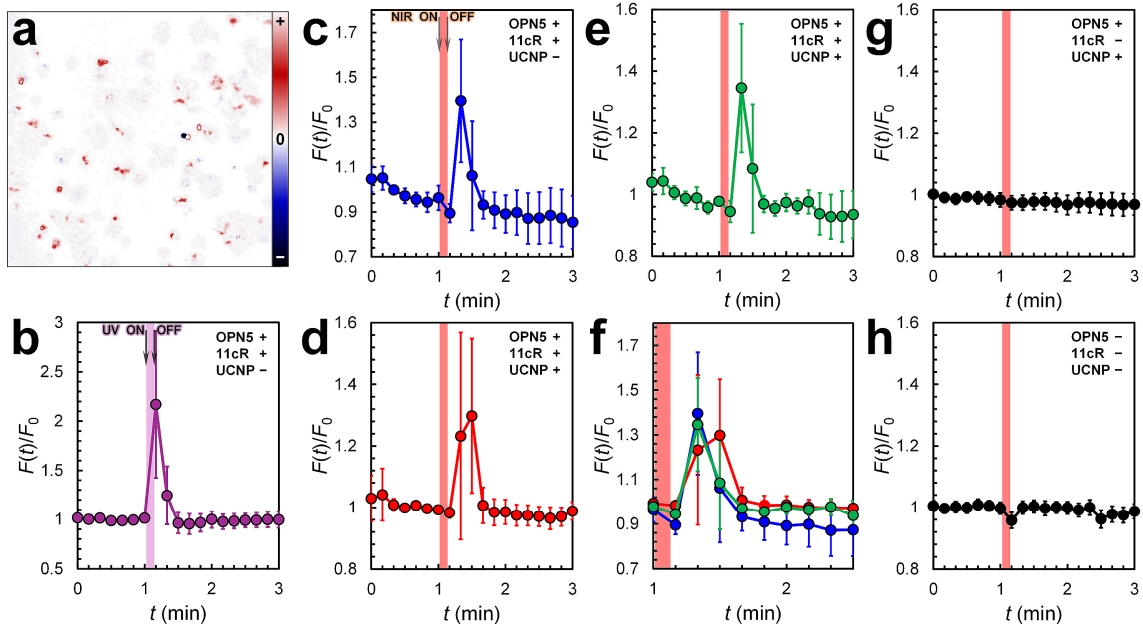


Figure S8. Results of the third replication experiment for Ca^{2+} imaging. (a) Difference fluorescence images before and after UV irradiation of OPN5-HEK (after – before). Note that the post-irradiation fluorescence image refers to the fluorescence image captured 1 second after the completion of UV irradiation. (b) \bar{F} when OPN5-HEK (-UCNP) was irradiated with UV light, (c) \bar{F} when OPN5-HEK (-UCNP) was irradiated with NIR light, (d) \bar{F} when OPN5-HEK (+UCNP (bound)) was irradiated with NIR light, and (e) \bar{F} when OPN5-HEK (+UCNP (unbound)) was irradiated with NIR light. (f) Graph plotted by overlaying panels c-e. (g) Average $F(t)/F_0$ for 100 randomly-selected cells in OPN5-HEK (+UCNP (bound), -11cR) when irradiated with NIR light ($N_{\text{responding}} = 0$), and (h) average $F(t)/F_0$ for 100 randomly-selected cells in HEK293T cells when irradiated with NIR light ($N_{\text{responding}} = 0$).

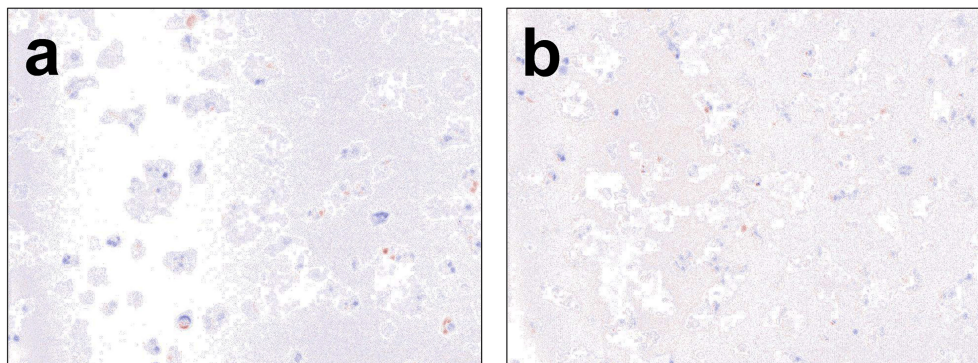


Figure S9. Typical difference fluorescence images before and after NIR light irradiation of OPN5-HEK (after – before) in (a) **Case 2** and (b) **Case 4**. Note that the post-irradiation fluorescence image refers to the fluorescence image captured 11 seconds after the completion of NIR light irradiation.

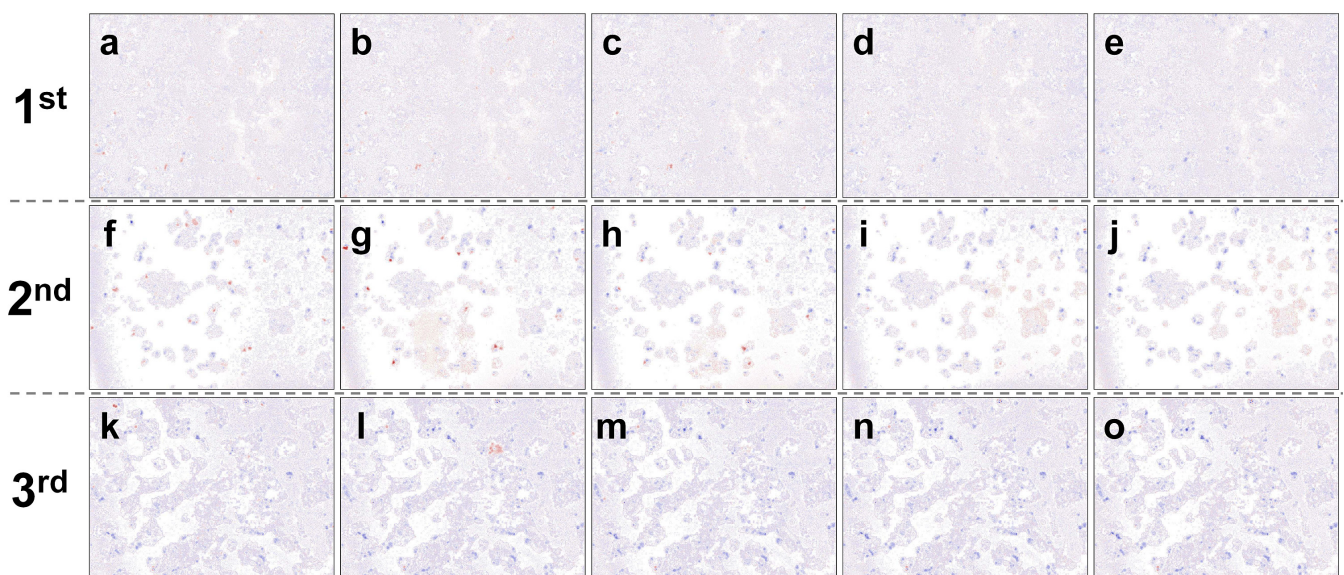


Figure S10. Difference fluorescence images before and after NIR light irradiation of OPN5-HEK (after – before) in **Case 3**. Results of (a-e) the first, (f-j) the second and (k-o) the third replication experiments. Difference fluorescence images were obtained by subtracting the pre-irradiation fluorescence image from the fluorescence image acquired after a specified time following completion of NIR light irradiation: (a,f,k) 11 seconds later, (b,g,l) 21 seconds later, (c,h,m) 31 seconds later, (d,i,n) 41 seconds later, and (e,j,o) 51 seconds later.

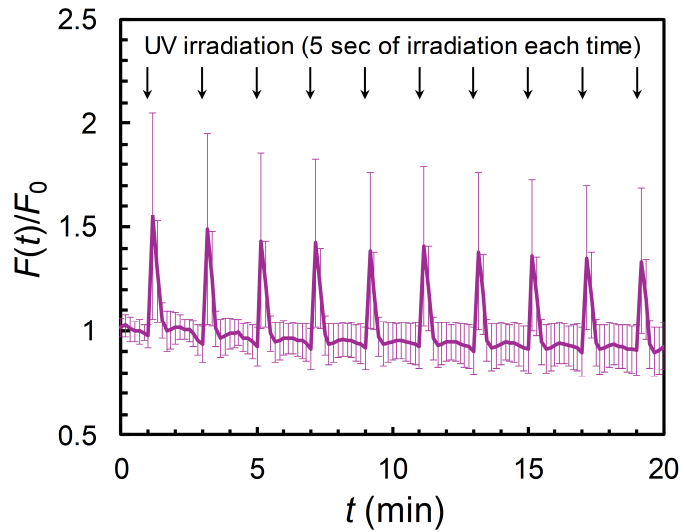


Figure S11. Ca^{2+} response of OPN5-HEK when intermittently irradiated with UV light (time for each irradiation: 5 sec). Note that the maximum value of $F(t)/F_0$ is smaller and the error bars are larger than in Figure 3b because this graph is the average of 100 randomly selected cells including non-responding cells.

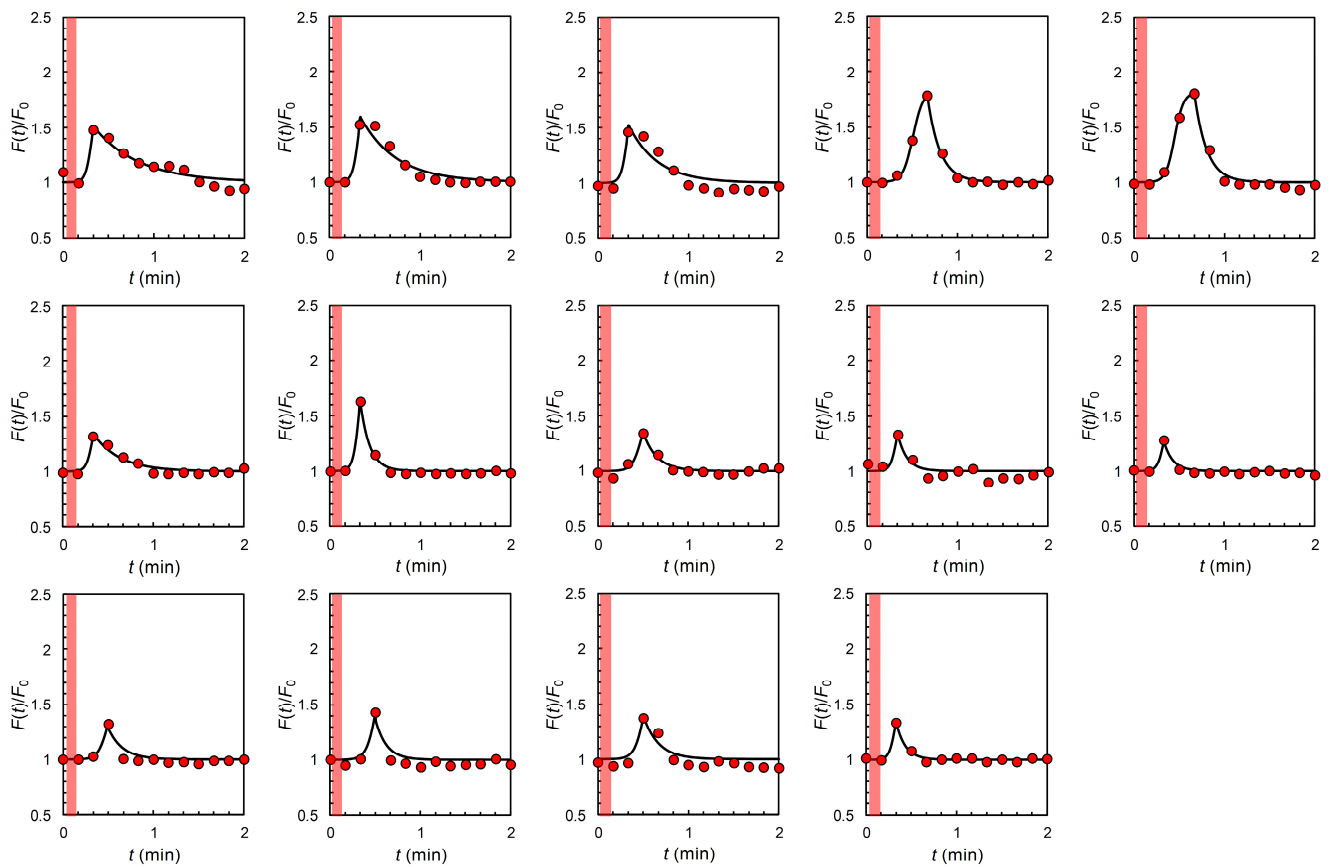


Figure S12. The time course of $F(t)/F_0$ for all responding cells in **Case 3** (plotted from 1 min after the start of fluorescence image acquisition). Regarding **Case 3**, the same experiment was repeated three times. For reference, the results of the first experiment are shown here. The red circles are the experimental data, the black lines are the fitting curves, and the red bands in each figure is the time during which NIR light was irradiated.

Table S1. $N_{\text{responding}}$, P_{res} , the number of cells with r_{low} , the number of cells with r_{mid} , and the number of cells with r_{high} in each of the three replication experiments.

Case	$N_{\text{responding}}$			$P_{\text{res}} (\%)$			Number of cells with r_{low}			Number of cells with r_{mid}			Number of cells with r_{high}		
	1 st	2 nd	3 rd	1 st	2 nd	3 rd	1 st	2 nd	3 rd	1 st	2 nd	3 rd	1 st	2 nd	3 rd
1	68	84	71	56.7	70.0	59.2	0	0	0	0	0	0	68	84	71
2	7	3	8	5.8	2.5	6.7	0	0	0	7	3	8	0	0	0
3	14	18	22	11.7	15.0	18.3	6	9	12	8	9	10	0	0	0
4	7	2	4	5.8	1.7	3.3	0	0	0	7	2	4	0	0	0
5	0	1	0	0.0	0.0	0.0	0	0	0	0	1	0	0	0	0
6	0	0	0	0.0	0.0	0.0	0	0	0	0	0	0	0	0	0

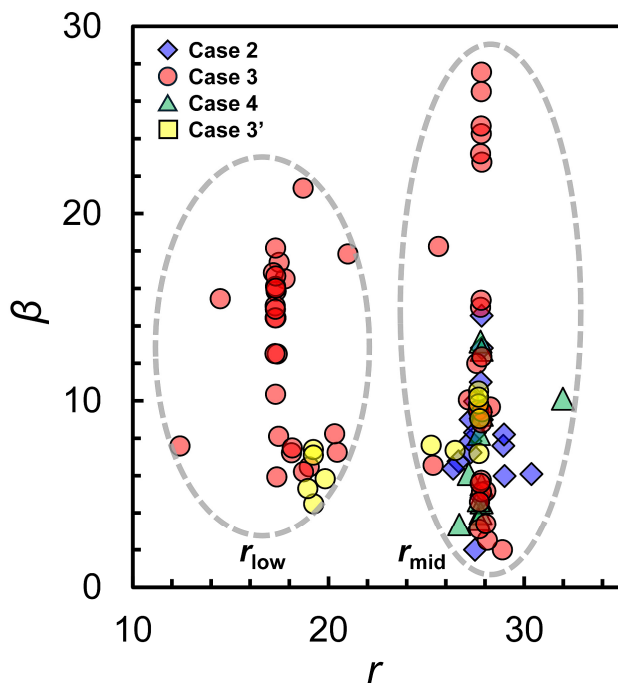


Figure S13. Phase diagram of r and β in **Cases 2 to 4**, with the phase diagram of **Case 3'** (yellow) added. The ratio of the number of cells with r_{low} to the number with r_{mid} ($N_{\text{low}}/N_{\text{mid}}$) in **Case 3'** was almost the same as $N_{\text{low}}/N_{\text{mid}}$ in **Case 3**, demonstrating high reproducibility. Note that **Case 3'** had a higher cell seeding density than **Case 3** (2.8×10^5 cells/dish), and accordingly, the amounts of plasmid and Lipofectamine 2000 added were changed to 0.56 $\mu\text{g}/\text{dish}$ and 1.12 $\mu\text{L}/\text{dish}$, respectively. The key point here is that cells belonging to the r_{low} group always appear at a certain proportion when UCNPs@Biotin was conjugated to OPN5-HEK and exposed to NIR irradiation, indicating that cells with activated OPN5 are always present due to the emission of UCNPs bound to the cells.

A brief explanation of the differences in P_{res} seen in Cases 1 to 4

For **Cases 1-4**, $N_{\text{responding}}$ can be written by the following equations, respectively:

$$N_{\text{responding}} = N_{\text{available}} \times p_n \times p_{e_{\text{UV}}} \quad (\text{Case 1})$$

$$N_{\text{responding}} = N_{\text{available}} \times p_n \times p_{e_{\text{NIR}}} \quad (\text{Case 2})$$

$$N_{\text{responding}} = N_{\text{available}} \times p_n \times (p_{e_{\text{NIR}}} + p_b \times p_{e_{\text{UCNP}}}) \quad (\text{Case 3})$$

$$N_{\text{responding}} = N_{\text{available}} \times p_n \times (p_{e_{\text{NIR}}} + p_{e_{\text{UCNP}}}) \quad (\text{Case 4})$$

where p_n , p_e and p_b respectively represent the probability of the presence of a normally functioning OPN5, the probability of the stimulus light reaching the OPN5 and causing its activation (taking into account the possibility that the photon may not reach the OPN5 due to absorption, scattering, refraction, *etc.*), and the probability of UCNP@Biotin binding to FLAG. The subscript of p_e represents the type of stimulus light.

In **Case 1**, $N_{\text{responding}}/N_{\text{available}} = 0.62$, so if we assume $p_{e_{\text{UV}}} = 1$, then $p_n = 0.62$. In **Case 2**, $N_{\text{responding}}/N_{\text{available}} = 0.05$, so if we use $p_n = 0.62$, then $p_{e_{\text{NIR}}} = 0.08$. In **Case 3**, $N_{\text{responding}}/N_{\text{available}} = 0.15$, so $p_b \times p_{e_{\text{UCNP}}} = 0.16$ is obtained. For example, if $p_b = 0.5$, then $p_{e_{\text{UCNP}}} = 0.32$, and if $p_b = 1$, then $p_{e_{\text{UCNP}}} = 0.16$. In any case, $p_{e_{\text{UCNP}}} > p_{e_{\text{NIR}}}$. In contrast, in **Case 4**, $p_{e_{\text{UCNP}}} = 0$ because $N_{\text{responding}}/N_{\text{available}} = 0.036$. These probabilities seem to be realistic values.

In **Case 3'** the number of cells seeded was 2.8 times (and the amount of UCNPs added approximately 4 times) that of **Case 3**. Since $N_{\text{responding}}/N_{\text{available}} = 0.1$, if p_n , $p_{e_{\text{NIR}}}$, and $p_{e_{\text{UCNP}}}$ are exactly the same values as in **Case 3**, $p_b'/p_b = 0.5$ where p_b' represents p_b in **Case 3'**. Therefore, it can be inferred that p_b' in **Case 3'** decreased to approximately 50% of p_b in **Case 3** for some reason, leading to a reduction in P_{res} to 10% ($P_{\text{res}} = 15\%$ in **Case 3**). Furthermore, the ratio of the number of cells with r_{low} to the number with r_{mid} ($N_{\text{low}}/N_{\text{mid}}$) in **Case 3'** was approximately 0.7 ($N_{\text{low}}/N_{\text{mid}} = 0.98 \pm 0.22$ in **Case 3**). $N_{\text{low}}/N_{\text{mid}}$ can be considered to be equal to $p_b \times p_{e_{\text{UCNP}}} / p_{e_{\text{NIR}}}$. Therefore, $p_b'/p_b = 0.58-0.92$. As mentioned above, the value of p_b'/p_b estimated from the P_{res} values is 0.5. Considering the variation in $p_{e_{\text{NIR}}}$ and $p_{e_{\text{UCNP}}}$ as well as experimental errors, this difference is believed to be within the acceptable range. Therefore, the slight decrease in $N_{\text{low}}/N_{\text{mid}}$ in **Case 3'** may be due to a slight decrease in the probability of UCNP@Biotin binding to FLAG when compared to **Case 3**.

REFERENCES

1. D. Kojima, S. Mori, M. Torii, A. Wada, R. Morishita and Y. Fukada, *PLoS One*, 2011, **6**, e26388.
2. N. T. Nguyen, J. Kim, X. T. Le, W. T. Lee, E. S. Lee, K. T. Oh, H.-G. Choi and Y. S. Youn, *ACS Nano*, 2023, **17**, 382–401.
3. D. Maemura, T. S. Le, M. Takahashi, K. Matsumura and S. Maenosono, *ACS Appl. Mater. Interfaces*, 2023, **15**, 42196–42208.
4. T. S. Le, M. Takahashi, N. Isozumi, A. Miyazato, Y. Hiratsuka, K. Matsumura, T. Taguchi and S. Maenosono, *ACS Nano*, 2022, **16**, 885–896.
5. M. Brown, L. J. Stafford, D. Onisk, T. Joaquim, A. Tobb, L. Goldman, D. Fancy, J. Stave and R. Chambers, *PLoS One*, 2013, **8**, e73255.
6. J. Hallgren, K. D. Tsirigos, M. D. Pedersen, J. J. Almagro Armenteros, P. Marcatili, H. Nielsen, A. Krogh and O. Winther, *bioRxiv*, 2022. DOI: 10.1101/2022.04.08.487609
7. W. S. Pear, G. P. Nolan, M. L. Scott and D. Baltimore, *Proc. Natl. Acad. Sci. U. S. A.*, 1993, **90**, 8392–8396.